Received: 13 February 2020 | Revised: 10 June 2020 | Accepted: 30 July 2020

DOI: 10.4218/etrij.2020-0053

ORIGINAL ARTICLE

ETRI Journal WILEY

Real-time implementation of distributed beamforming for simultaneous wireless information and power transfer in interference channels

Yong-Gi Hong | **SeongJun Hwang** | **Jiho Seo** | **Jonghyeok Lee** | **Jaehyun Park**

Department of Electronic Engineering, Pukyong National University, Busan, Rep. of Korea

Correspondence
Jaehyun Park, Pukyong National University, Busan, Rep. of Korea.
Email: jaehyun@pknu.ac.kr

Funding information
This work is supported by the Basic Science Research Program through the National Research Foundation of Korea funded by the Ministry of Education (2018R1D1A1B07043786).

[Correction added on 22nd December 2020, after first online publication: The images in the author biographies have been matched with the correct authors.]

In this paper, we propose one-bit feedback-based distributed beamforming (DBF) techniques for simultaneous wireless information and power transfer in interference channels where the information transfer and power transfer networks coexist in the same frequency spectrum band. In a power transfer network, multiple distributed energy transmission nodes transmit their energy signals to a single energy receiving node capable of harvesting wireless radio frequency energy. Here, by considering the Internet-of-Things sensor network, the energy harvesting/information decoding receivers (ERx/IRx) can report their status (which may include the received signal strength, interference, and channel state information) through one-bit feedback channels. To maximize the amount of energy transferred to the ERx and simultaneously minimize the interference to the IRx, we developed a DBF technique based on one-bit feedback from the ERx/IRx without sharing the information among distributed transmit nodes. Finally, the proposed DBF algorithm in the interference channel is verified through the simulations and also implemented in real time by using GNU radio and universal software radio peripheral.

KEYWORDS
distributed beamforming, GNU-Radio, interference channel, SWIPT, USRP

1 | INTRODUCTION

The manufacturing industry is moving toward the fourth industrial revolution (eg, Industry 4.0) and, as a key application in Industry 4.0, a smart factory exploits Internet of things (IoT) technologies that connect devices and enable their autonomous data exchange (see [1,2] and the references therein). Specifically, an IoT wireless sensor network is being studied in the form of a massive sensor network composed of a large number of small sensor nodes. However, because the sensor nodes are battery limited, the power management of these massive sensor nodes becomes a critical issue for deploying a massive IoT sensor network. To overcome the energy depletion in massive IoT sensor networks, the deployment of the senor nodes capable of harvesting radio frequency (RF) energy wirelessly has been considered [3,4].

In particular, since existing wireless RF communication signals can be used as a source for energy harvesting [5,6], research on transmission strategies about simultaneous wireless information and power transfer (SWIPT) has been extensively investigated [6–9]. Because the energy signal has different impacts on the performances of the information

decoding receiver (IRx; ie, a negative impact) and energy harvesting receiver (ERx; ie, a positive impact), the design of suitable transmission strategies for SWIPT is a critical issue, especially in an interference channel, where the information transfer network and the power transfer network coexist in the same frequency spectrum band. Most previous studies have investigated the fundamental performance limits and the optimal transmission strategies of the SWIPT with perfect channel state information at the transmitter (CSIT), theoretically [7–9].

In this paper, by considering the IoT sensor network, where the information transfer network and the power transfer network coexist in the same frequency spectrum band, we propose distributed energy beamforming strategies for multiple energy transmitters (ETxs) based on one-bit feedback from the ERx and IRx. Specifically, the ERx and IRx can report their status (which may include the received signal strength, interference, and channel state information) through one-bit feedback channels. Here, to maximize the amount of energy transferred to the ERx and, at the same time, minimize the interference to the IRx, we develop distributed beamforming (DBF) techniques based on one-bit feedback from the ERx/IRx without sharing information among the distributed energy transmit nodes. DBF techniques [10] have been widely considered to improve system performance without increasing system complexity, where the spatially distributed transmitters adjust their phases to synchronize the received signal at the desired receiver. Furthermore, considering the IoT sensor network, the receiver can only impart a one-bit feedback report instead of an accurate channel estimate to each transmitter. Accordingly, DBF algorithms based on one-bit feedback have been investigated in [11–14]. Different from previous work, in this paper, we consider an interference channel in which the information transfer network and the energy transfer network coexist and accordingly, the two different impacts of DBF on the ERx and IRx should be considered. Accordingly, we developed a DBF strategy maximizing the harvested energy at the ERx and DBF strategy minimizing the interference at the IRx. We also propose a DBF jointly maximizing the energy transferred to the ERx and minimizing the interference at the IRx in a stochastic way, where multiple ETxs determine their phases of the energy signal based on one-bit feedback reports from the ERx/IRx without sharing information among the distributed transmit nodes. Note that when the energy transferred to the ERx is maximized, the interference at the IRx tends to increase. In addition, when the interference is minimized at the IRx, the energy transferred to the ERx tends to decrease. Accordingly, there exists a trade-off between the energy maximization and the interference minimization. Through computer simulations, we identify the trade-off between the transferred energy and the achievable rate. Based on this trade-off curve, we can also propose the optimal transmission strategy such that the harvested energy at the ERx is maximized without sacrificing the achievable rate at the IRx. Finally, the proposed DBF algorithms in the interference channel are implemented in real time using GNU radio [15], universal software radio peripheral (USRP) [16], and a P2110 board with a rectenna [17]. Considering a SWIPT implementation with one-bit feedback in the interference channel for the first time, the contributions of this paper are listed below:

1. To manage two different impact of the energy signals in a distributed way, we first develop two different distributed energy beamforming strategies for multiple ETxs based on one-bit feedback from the ERx and IRx in the interference channel. First, the distributed nodes adjust their transmit signal phase based on one-bit feedback from the ERx to maximize the energy transferred to the ERx, which is equivalent to the conventional signal to noise ratio (SNR) maximizing DBF [11–14]. Second, we also develop the DBF based on one-bit feedback from the IRx that minimizes the interference at the IRx.
2. To maximize the transferred energy and simultaneously minimize the interference, a new DBF is also proposed, where the distributed nodes update their phases based on the feedback from both the ERx and IRx in a stochastic way. Note that the priority between the transferred energy and the achievable rate can be adjusted by changing the phase update probability in the proposed algorithm.
3. Through computer simulations, the trade-off between the transferred energy and the achievable rate is identified. We note that the proposed DBF jointly maximizing the energy transferred to the ERx and minimizing the interference at the IRx outperforms the orthogonal time-sharing between the energy maximizing DBF and the interference minimizing DBF.
4. The proposed DBF algorithms in the interference channel are experimentally verified through a real-time implementation using GNU radio [15], USRP [16], and a P2110 board with a rectenna [17]. From the experimentally obtained measurements, we confirm that the proposed DBF can effectively increase the energy transferred to the ERx and simultaneously decrease the interference at the IRx. We also note that the real-time implementation of DBF in the interference channels, where the information transfer network and the energy transfer network share the same frequency band, has not yet been handled in the open literature, to the best of our knowledge. Furthermore, when the proposed scheme is exploited, the IRx and ERx nodes do not need complex transceiver structures for the feedforward/feedback channels.

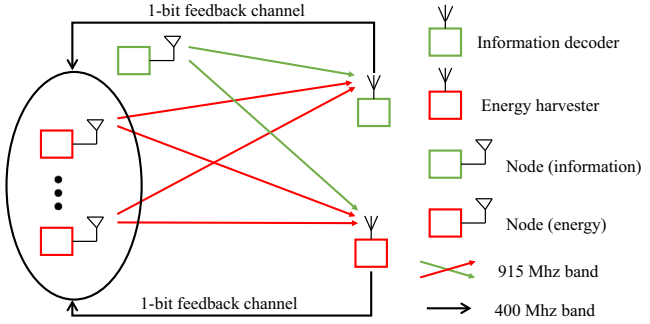

FIGURE 1 SWIPT in the interference channel where the information transceiver and energy transceiver coexist, exploiting the same RF spectrum band

The rest of this paper is organized as follows. In Section 2, we introduce the SWIPT model in the interference channel. In Section 3, we propose DBF algorithms with one-bit feedback considering both the harvested energy at the ERx and the achievable rate at the IRx. In Section 4, we provide several simulation results, and in Section 5, we present the real-time implementation of our proposed DBF system. In Section 6, we give our conclusion.

2 | SYSTEM MODEL

In Figure 1, we consider SWIPT in the interference channel where a single information transmit node (ITx) and N distributed ETxs transmit the information/energy signals to their associated IRx/ERx through the same RF spectrum band.[1] When each node is equipped with a single antenna, the nth ETx signal at the ith time slot can be expressed as.

$$s_n[i] = A_n[i]e^{j(\phi_n+\theta_n[i])}, \tag{1}$$

where $A_n[i]$ is the nth ETx signal waveform and ϕ_n is the phase offset at the local oscillator of the nth ETx. In addition, $\theta_n[i]$ is an adjustable transmit phase at the nth ETx. Throughout the paper, we assume that $A_1[i] = \cdots = A_N[i] = A[i]$. Likewise, the ITx signal at the ith time slot can be expressed as

$$s_I[i] = B_I[i]e^{j\phi_I}, \tag{2}$$

where $B_I[i]$ is the information-carrying modulated symbol and ϕ_I is the phase offset at the local oscillator of the ITx. Therefore, the received signal at the ERx can be expressed as follows.

$$\begin{aligned} r_E[i] &= \sum_{n=1}^{N} h_{En}s_n[i] + h_{E0}s_I[i] + n_E[i] \\ &= \sum_{n=1}^{N} r_{En}A[i]e^{j(\phi_n+\psi_{En}+\theta_n[i])} + h_{E0}s_I[i] + n_E[i], \end{aligned} \tag{3}$$

where $h_{En} = r_{En}e^{j\psi_{En}}$(respectively, h_{E0}) is the channel gain between the nth ETx (respectively, the ITx) and the ERx with $r_{En} \geq 0$, $\psi_{En} \in [0, 2\pi]$, $n = 0, \ldots, N$. Here, h_{En} and h_{E0} are independent and identically distributed zero-mean complex Gaussian random variables with variances σ_{En}^2 and σ_{E0}^2, respectively, and n_E is the additive Gaussian noise with a variance σ_n^2. Throughout the paper, the block fading is assumed where the channel state remains quasi-static within a fading block, which is commonly used assumption in wireless communications [18–20]. Likewise, the received signal at the IRx can be expressed as

$$\begin{aligned} r_I[i] &= h_{I0}s_I[i] + \sum_{n=1}^{N} h_{In}s_n[i] + n_I[i] \\ &= h_{I0}B_I[i]e^{j\phi_I} + \sum_{n=1}^{N} r_{In}A[i]e^{j(\phi_n+\psi_{In}+\theta_n[i])} + n_I[i], \end{aligned} \tag{4}$$

where $h_{In} = r_{In}e^{j\psi_{In}}$(respectively, h_{I0}) is the channel gain between the n th ETx (respectively, the ITx) and the IRx with $r_{In} \geq 0$, $\psi_{In} \in [0, 2\pi]$, $n = 0, \ldots, N$. Again, h_{In} and h_{I0} are independent and identically distributed zero-mean complex Gaussian random variables with variances σ_{In}^2 and σ_{I0}^2, respectively, and n_I is the additive Gaussian noise with a variance σ_n^2.

From (3), the instantaneous energy collected at the ERx in the ith time slot can be expressed as follows.

$$\begin{aligned} E_{\text{harv}}[i] &= \eta T_s \left|r_E[i]\right|^2 \\ &\approx \eta T_s A^2[i] \left|\sum_{n=1}^{N} r_{En}^2 e^{j(\phi_n+\psi_{In}+\theta_n[i])}\right|^2, \end{aligned} \tag{5}$$

where η represents the energy conversion efficiency and T_s is the time slot period. Note that, to harvest enough energy at the ERx, the distance between the ETxs and ERx is generally smaller than that between the ITx and ERx (ie, $\sigma_{En}^2 \gg \sigma_{E0}^2$), resulting in the approximation in (5). We note that the harvested energy in (5) is also proportional to the received signal strength (RSS).

From (4), the instantaneously received SINR at the IRx can be calculated as

$$\text{SINR}[i] = \frac{\left|r_{I0}B_I[i]\right|^2}{\left|A[i]\sum_{n=1}^{N} r_{In}e^{j(\phi_n+\psi_{In}+\theta_n[i])}\right|^2 + \sigma_n^2}. \tag{6}$$

Accordingly, the achievable rate at the IRx can be given as

$$\text{Rate}_{\text{IRx}}[i] = \log_2(1 + \text{SINR}[i]). \tag{7}$$

[1]Throughout the paper, we consider the scenario with one ITx and multiple ETxs to overcome the limited RF harvesting efficiency through the DBF, but the proposed scheme can be extended to a scenario with multiple ITx and multiple ETx nodes [7].

3 | DISTRIBUTED BEAMFORMING STRATEGIES WITH ONE-BIT FEEDBACK

3.1 | DBF maximizing the energy transferred to the ERx

To maximize the harvested energy at the ERx, the energy signals from multiple ETxs need to be coherently received at the ERx. However, because we consider an IoT sensor network, we assume that there is no cooperation among the ETxs with no CSIT. Worse, there exists a one-bit feedback channel from the ERx to the ETxs. One approach is that the phases of the ETxs can be adjusted by applying a one-bit feedback-based random gradient search method such that the phases of the energy signals are aligned to maximize the transferred energy to the ERx [12] (ie, $\phi_n + \psi_{En} + \theta_n[i] = C$ for $n = 1, \ldots, N$). More specifically, the ERx sends feedback bit "1" if the current RSS, which is proportional to the harvested energy, is greater than the previous RSS. Otherwise, it sends bit "0." Based on the received feedback bit, the ETxs can decide whether to update their optimal phase $\theta_{\text{best},n}$ as $\theta_n[i]$. The next phase $\theta_n[i+1]$ is then determined by adding a small perturbation on the current optimal phase $\theta_{\text{best},n}$. The process explained above is summarized in Algorithm 1.

Algorithm 1 DBF maximizing the energy transferred to the ERx

1. Initialization

At the ETxs: The optimal phase of the n th ETx, $\theta_{\text{best},n}$, is initialized randomly according to the uniform distribution on $[-\pi, \pi]$ and the energy signal is transmitted with $\theta_n[1] = \theta_{\text{best},n}$ in the first time slot. Set $i_{\text{converge}} = 0$.

At the ERx: The energy is harvested during the first time slot and the associated RSS is stored as $Y_{\text{best}} = |r_E[1]|$, and a feedback bit "1" is transmitted via the feedback channel.

2. Updating phase & deciding feedback bit for $i = 2$: $N_{\max}$

At the ETxs: When feedback bit "1" is received, the optimal phase of each node $\theta_{\text{best},n}$ is updated as $\theta_{\text{best},n} = \theta_n[i-1]$. Otherwise, $\theta_{\text{best},n}$ is not updated and $i_{\text{converge}} = i_{\text{converge}} + 1$.

If $i_{\text{converge}} \geq I_{\text{threshold}}$ with a fixed constant $I_{\text{threshold}}$, then terminate the algorithm.

The energy signal is then transmitted with

$\theta_n[i] = \theta_{\text{best},n} + \delta$,,

where δ is the small perturbation following the uniform distribution over $[-\Delta, \Delta]$. Set Δ as $\pi/20$.

At the ERx: The RSS in the i th time slot (ie, $Y[i] = |r_E[i]|$) is measured and the feedback bit and the optimal RSS are respectively determined as

feedbackbit $= '1'$ and $Y_{\text{best}} = Y[i]$ if $Y[i] > Y_{\text{best}}$;

feedbackbit $= '0'$ and $Y_{\text{best}} = Y_{\text{best}}$ otherwise.

We note that in Step 2 of Algorithm 1, the iteration can be terminated when the feedback bit "0" is received more than $I_{\text{threshold}}$ times consecutively (equivalently, the RSS at the ERx has converged). That is, if each Tx receives the feedback bits of consecutive zeroes, i_{converge} increases to $I_{\text{threshold}}$ (which was set to 200 in our simulations, but can be determined empirically) and it is determined that the optimal point has been reached, the algorithm can be terminated.

3.2 | DBF minimizing the interference at the IRx

To minimize the interference at the IRx, the energy signals from multiple ETxs need to be destructively superposed at the IRx. That is, the phases of multiple ETxs should be adjusted in a distributed way so that the RSS of the interference at the IRx is minimized.[2] Similarly to how DBF maximizes the harvested energy at the ERx, we can develop a one-bit feedback-based random gradient search method. Specifically, the IRx sends feedback bit "1" if the current RSS of interference, which is inversely proportional to the achievable rate, is smaller than the previous RSS of the interference. That is, smaller interference power is better for the achievable rate. Otherwise, it sends bit "0." Accordingly, DBF minimizing the interference at the IRx can be summarized as Algorithm 2.

Algorithm 2 DBF minimizing the interference at the IRx

1. Initialization

At the ETxs: The optimal phase of the n th ETx $\theta_{\text{best},n}$ is initialized randomly according to the uniform distribution on $[-\pi, \pi]$ and the energy signal is transmitted with $\theta_n[1] = \theta_{\text{best},n}$ in the first time slot.

At the IRx: The RSS of the interference is stored as $I_{\text{best}} = |r_I[1] - h_{I0}s_I[1]|$, and a feedback bit "1" is transmitted via the feedback channel.

2. Updating phase & deciding feedback bit for $i = 2$: $N_{\max}$

At the ETxs: When feedback bit "1" is received, the optimal phase of each node $\theta_{\text{best},n}$ is updated as $\theta_{\text{best},n} = \theta_n[i-1]$. Otherwise, $\theta_{\text{best},n}$ is not updated and $i_{\text{converge}} = i_{\text{converge}} + 1$.

If $i_{\text{converge}} \geq I_{\text{threshold}}$ with a fixed constant $I_{\text{threshold}}$, then terminate the algorithm.

The energy signal is then transmitted with $\theta_n[i] = \theta_{\text{best},n} + \delta$.

At the IRx: The RSS of the interference in the i th time slot (ie, $I[i] = |r_I[i] - h_{I0}s_I[i]|$) is measured and the feedback bit and the optimal RSS of interference are respectively determined as

feedbackbit $= '1'$ and $I_{\text{best}} = I[i]$ if $I[i] < I_{\text{best}}$;

feedbackbit $= '0'$ and $Y_{\text{best}} = Y_{\text{best}}$ otherwise.

[2]We note that the interference power (or RSS of the interference) can be estimated by subtracting the desired signal power from the received power, where the desired signal power can be estimated during the frame synchronization process with known preamble signals at the beginning of the coherent information data transmission block.

We note that in Step 2 of Algorithm 2, the iteration can be terminated when the interference power at the IRx has converged.

3.3 | DBF jointly maximizing the energy transferred to the ERx and minimizing the interference at the IRx

Because the energy signal has two different impacts on the performances of the ERx and IRx (ie, the energy signal strength is maximized at the ERx while it is minimized at the IRx), multiple ETxs can choose their phases based on one-bit feedback reports from the ERx and IRx.[3] Specifically, from Algorithms 1 and 2, if both the ERx and IRx send feedback bit "1" (which implies that the current RSS is greater than the previous RSS at the ERx and simultaneously, the current interference is smaller than the previous interference at the IRx), they update their optimal phase $\theta_{\text{best},n}$ as $\theta_n[i]$. If both the ERx and IRx send feedback bit "0" (which implies that the current RSS is not increased compared to the previous RSS at the ERx and simultaneously, the current interference is not decreased at the IRx), they do not update their optimal phase $\theta_{\text{best},n}$ as $\theta_n[i]$. When the ERx and IRx send different feedback bits, each ETx updates its optimal phase $\theta_{\text{best},n}$ as $\theta_n[i]$ with a probability P_{update}. According to the feedback bits, the update of $\theta_{\text{best},n}$ is summarized in Table 1.

From Table 1, if $P_{\text{update}} = 1$, the phase $\theta_{\text{best},n}$ is updated according to the feedback bit from the ERx without considering that from the IRx, and vice versa. Accordingly, Algorithm 1 (respectively, Algorithm 2) can be regarded as a special case of Algorithm 3 with $P_{\text{update}} = 1$ (respectively, $P_{\text{update}} = 0$). That is, Algorithm 3 with $P_{\text{update}} = 1$ is equivalent to Algorithm 1, which maximizes the harvested energy at the ERx. In addition, Algorithm 3 with $P_{\text{update}} = 0$ is equivalent to Algorithm 2, which minimizes the interference at the IRx. Note that, even though Algorithms 1 and 2 can be explained as special cases of Algorithm 3, their simple combinations with time division multiple access (TDMA) or frequency division multiple access (FDMA) are inferior to Algorithm 3 with a proper P_{update}, which is validated in Section 4. We also note that P_{update} can be determined according to the priority between the information transfer and the energy transfer. More specifically, for a large P_{update}, the distributed nodes can update their phases in favor of the ERx. In contrast, for a small P_{update}, the nodes update their phases in favor of the IRx.

[3]For the sake of implementation simplicity, in our system model, orthogonal resource allocation such as TDMA is considered for one-bit channels from the ERx and IRx, but the superposition method could also be applied in the feedback channel.

TABLE 1 Update of $\theta_{\text{best},n}$ for DBF

Feedback bit from ERx	Feedback bit from the IRx	Update of $\theta_{\text{best},n}$
0	0	No update
0	1	$\theta_{\text{best},n} = \theta_n[i]$ with a probability $1 - P_{\text{update}}$
1	0	$\theta_{\text{best},n} = \theta_n[i]$ with a probability P_{update}
1	1	$\theta_{\text{best},n} = \theta_n[i]$

Algorithm 3 DBF jointly maximizing the energy transferred to the ERx and minimizing the interference at the IRx

1. Initialization

At the ETxs: The optimal phase of the n th ETx, $\theta_{\text{best},n}$, is initialized randomly according to the uniform distribution on $[-\pi, \pi]$ and the energy signal is transmitted with $\theta_n[1] = \theta_{\text{best},n}$ in the first time slot.

At the ERx: The energy is harvested during the first time slot and the associated RSS is stored as $Y_{\text{best}} = |r_E[1]|$, and a feedback bit "1" is transmitted via the feedback channel.

At the IRx: The RSS of the interference is stored as $I_{\text{best}} = |r_I[1] - h_{I0}s_I[1]|$, and a feedback bit "1" is transmitted via the feedback channel.

2. Updating phase & deciding feedback bit for $i = 2$: $N_{\max}$

At the ETxs: If the receiving feedback bits from the ERx and IRx are "11," the optimal phase of each node $\theta_{\text{best},n}$ is updated as $\theta_{\text{best},n} = \theta_n[i-1]$. Else if the receiving feedback are "01," $\theta_{\text{best},n}$ is updated as $\theta_{\text{best},n} = \theta_n[i-1]$ with a probability $1 - P_{\text{update}}$. Else if the receiving feedback are "10," $\theta_{\text{best},n}$ is updated as $\theta_{\text{best},n} = \theta_n[i-1]$ with a probability P_{update}. Otherwise, $\theta_{\text{best},n}$ is not updated and $i_{\text{converge}} = i_{\text{converge}} + 1$.

If $i_{\text{converge}} \geq I_{\text{threshold}}$ with a fixed constant $I_{\text{threshold}}$, then terminate the algorithm.

The energy signal is then transmitted with $\theta_n[i] = \theta_{\text{best},n} + \delta$.

At the ERx: The RSS in the i th time slot (ie, $Y[i] = |r_E[i]|$) is measured and the feedback bit and the optimal RSS are, respectively, determined as

$\text{feedbackbit} = '1'$ and $Y_{\text{best}} = Y[i]$ if $Y[i] > Y_{\text{best}}$;

$\text{feedbackbit} = '0'$ and $Y_{\text{best}} = Y_{\text{best}}$ otherwise.

At the IRx: The RSS of the interference in the i th time slot (ie, $I[i] = |r_I[i] - h_{I0}s_I[i]|$) is measured and the feedback bit and the optimal RSS of interference are, respectively, determined as

$\text{feedbackbit} = '1'$ and $I_{\text{best}} = I[i]$ if $I[i] < I_{\text{best}}$;

$\text{feedbackbit} = '0'$ and $Y_{\text{best}} = Y_{\text{best}}$ otherwise.

We note that in Step 2 of Algorithm 3, the iteration can be terminated when the RSS at the ERx is converged and, simultaneously, the interference power at the IRx is converged (ie, when the feedback bits "00" are received more than $I_{\text{threshold}}$ times consecutively).

4 | SIMULATION

To verify the proposed DBF for the interference channel, computer simulations were performed. Throughout the simulation, all nodes had a single antenna and we set $N = 6$ and SNR = 30 dB. In addition, the transmit power at each node was set as 100 mW and the path loss was 20 dB. The energy conversion efficiency was assumed to be 1, but it can be straightforwardly applicable to other values.

In Figures 2 and 3, the received signal power at the ERx and the achievable rate at the IRx are evaluated for DBF maximizing the harvested energy at the ERx (Algorithm 1) and DBF minimizing the interference at the IRX (Algorithm 2), respectively. It can be found that both the received signal power and the achievable rate converged after less than 3,000 iterations. In addition, the received signal power for the DBF maximizing the harvested energy at the ERx (ie, Algorithm 3 with $P_{\text{update}} = 1$) is higher than that for the DBF minimizing the interference at the IRx (ie, Algorithm 3 with $P_{\text{update}} = 0$). In contrast, the DBF minimizing the interference at the IRx shows a higher achievable rate. That is, we can see the trade-off between the harvested energy at the ERx and the achievable rate at the IRx.

Motivated by the above observation, in Figure 4, the trade-off curve (blue solid line) between the received signal power at the ERx and the achievable rate at the IRx is evaluated by exploiting Algorithm 3 with various values of P_{update}. For comparison purposes, we also evaluate the trade-off curve (red solid line) when Algorithm 1 and Algorithm 2 are simply combined with TDMA-based resource allocation. From the figure, we can find that a FDMA/TDMA-based merging of Algorithms 1 and 2 exhibits a worse trade-off curve than Algorithm 3 by controlling the update probability (P_{update}). In addition, from Figure 4, we can reduce P_{update} up to 0.7 to increase the energy transferred to the ERx without sacrificing the achievable rate at the IRx.

Figure 5 shows, the received signal power and the achievable rate is provided when Algorithm 3 with $P_{\text{update}} = 0.7$ is applied. We can see that Algorithm 3 with $P_{\text{update}} = 0.7$ exhibits much a higher harvested energy compared to that with Algorithm 2 (in Figure 3) without sacrificing the achievable rate performance. We note that one may propose some heuristic methods to cope with "01" and "10" feedback cases better, resulting in a better trade-off in Figure 4. We believe that Algorithm 3 with controllable P_{update} is simple and efficient to implement and, motivated by our proposed approach,

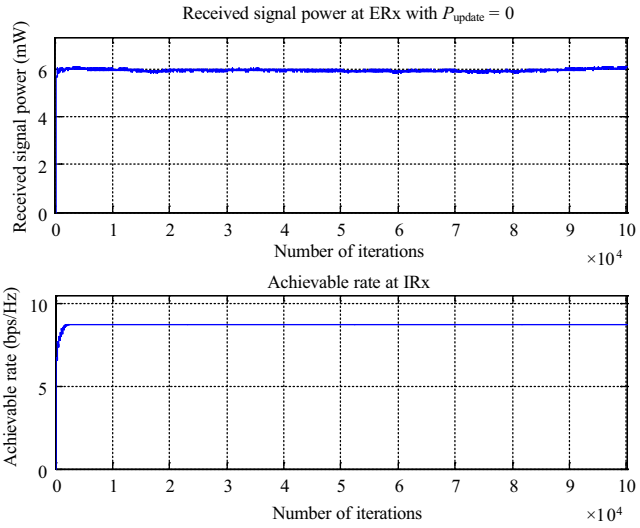

FIGURE 3 Received signal power at the ERx and achievable rate at the IRx when the DBF minimizing the interference at the IRx (Algorithm 2) is applied

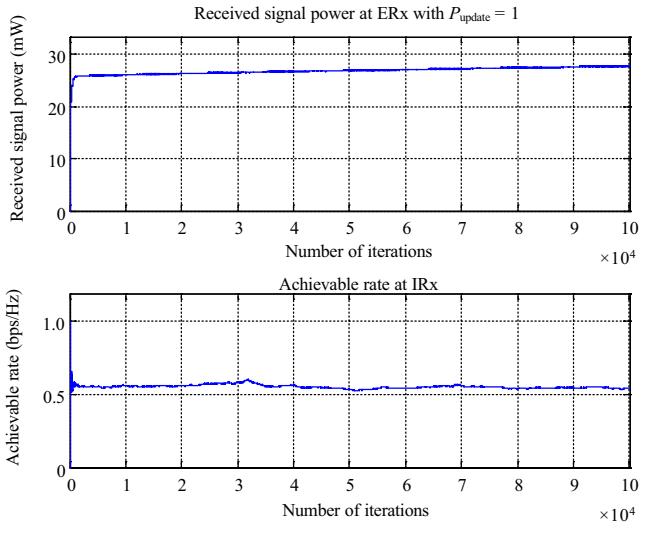

FIGURE 2 Received signal power at the ERx and achievable rate at the IRx when the DBF maximizing the harvested energy at the ERx (Algorithm 1) is applied

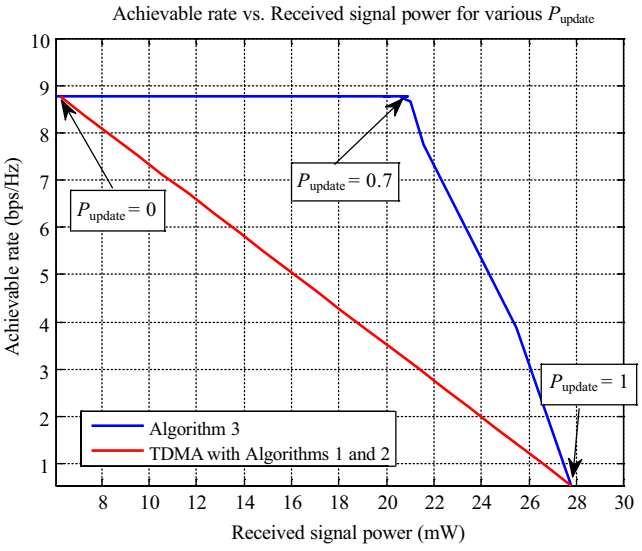

FIGURE 4 Received signal power at the ERx and achievable rate at the IRx when Algorithm 3 is applied with various values of P_{update}

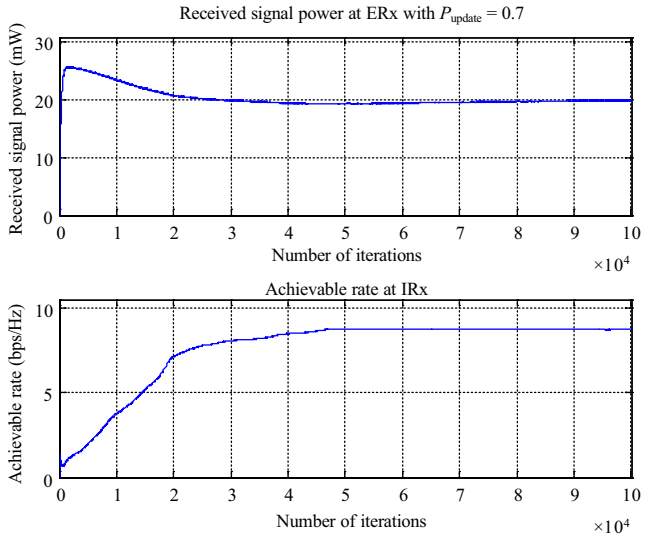

FIGURE 5 Received signal power at the ERx and achievable rate at the IRx when Algorithm 3 is applied with $P_{update} = 0.7$

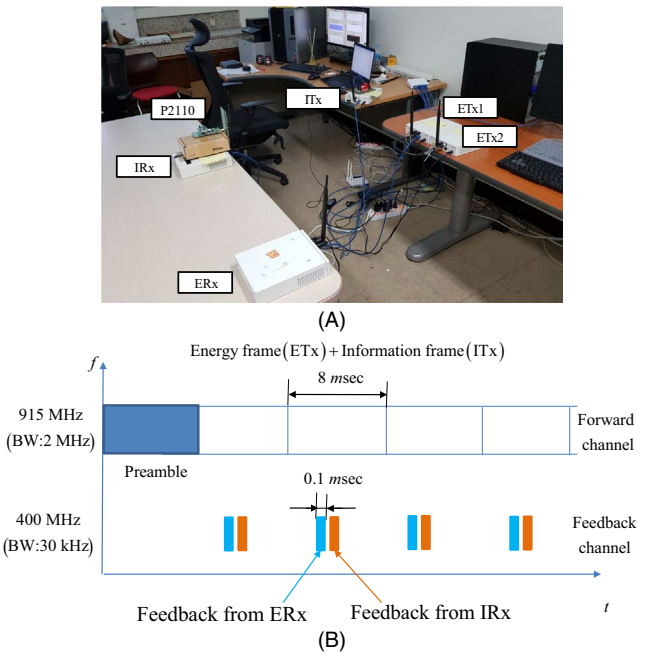

FIGURE 6 (A) Real-time implementation setup and (B) frame structures of the proposed DBF in the interference channel

some heuristic methods to improve the performance can be developed.

5 | REAL-TIME IMPLEMENTATION WITH GNU RADIO AND USRP

Figure 6 shows the real-time implementation setup (top) and the frame structures (bottom) for the proposed DBF in the interference channel, which is composed of multiple USRP N210 devices [16] with WBX boards, one host computer, and a P2110 board with a rectenna [17]. Specifically, all nodes including two ETxs, one ERx, one ITx, and one IRx were implemented with a USRP N210 with a WBX board, where the frequency band of 915 MHz is used for both the energy transfer and information transfer, each with a 2 MHz bandwidth. In addition, the feedback channel is allocated in the 400 MHz band with 30 kHz bandwidth. For the sake of the implementation simplicity, TDMA is exploited for the one-bit channels from the ERx and IRx. Detailed experimental parameters are listed in Figure 6 (bottom), but each parameter can be changed and tuned.

To validate the energy transfer, we measured the received signal strength at the USRP N210 energy receiver using a vertical antenna and measured the amount of harvested energy using the P2110 toolkit with a rectenna (an off-the-shelf energy harvesting device [17]), which is able to power an LED. To focus on the effect on the DBF algorithm through the phase adjustment, all the frequency offsets among the nodes are synchronized using the GPS disciplined oscillator (GPSDO). The ITx exploits quadrature phase shift keying (QPSK) modulation to transfer the information and the ETxs exploits a sinusoidal waveform to transfer the energy, while the on-off keying (OOK) is exploited in the feedback channel for simplicity of implementation. In Figure 6 (bottom), the orthogonal time slot allocation is implemented such that the time slot for the feedback from the ERx is first allocated and then the time slot for the feedback from the IRx follows. In the real-time experiment, we set the time interval between those two time slots to 2 ms to stably separate them.

In Figure 7, the flow graph of beamforming process at each ETx is presented, where multiple ETxs and one ERx (or one IRx) communicate, and the associated beamforming process is summarized as follows:

1. When the value of the received sample is higher than the "HIGH value" of the Threshold block, the Generatorblock is informed by the simple OOK receiver that the ERx (or IRx) sent bit "1" (Part 1 in Figure 7).
2. Based on the received feedback bit, the Generatorblock updates $\theta_{\text{best},n}$. In addition, a random perturbation value with a range of $[-\pi/20, \pi/20]$ is conveyed to the Generatorblock for the next phase determination, as in (8) (Part 2 in Figure 7).
3. Finally, the energy signal is transmitted from the USRP Sink block a the period of T_{tr} (Parts 3 and 4 in Figure 7).

In Figure 8, the GNU radio blocks for the ERx are shown. Note that the maxpowercheck block updates its Y_{best} every time slot. That is, if the energy of the current time slot is larger than the one saved before, it updates Y_{best}.

We implemented our information transmission system using QPSK modulation to transmit an audio file [21], as shown in

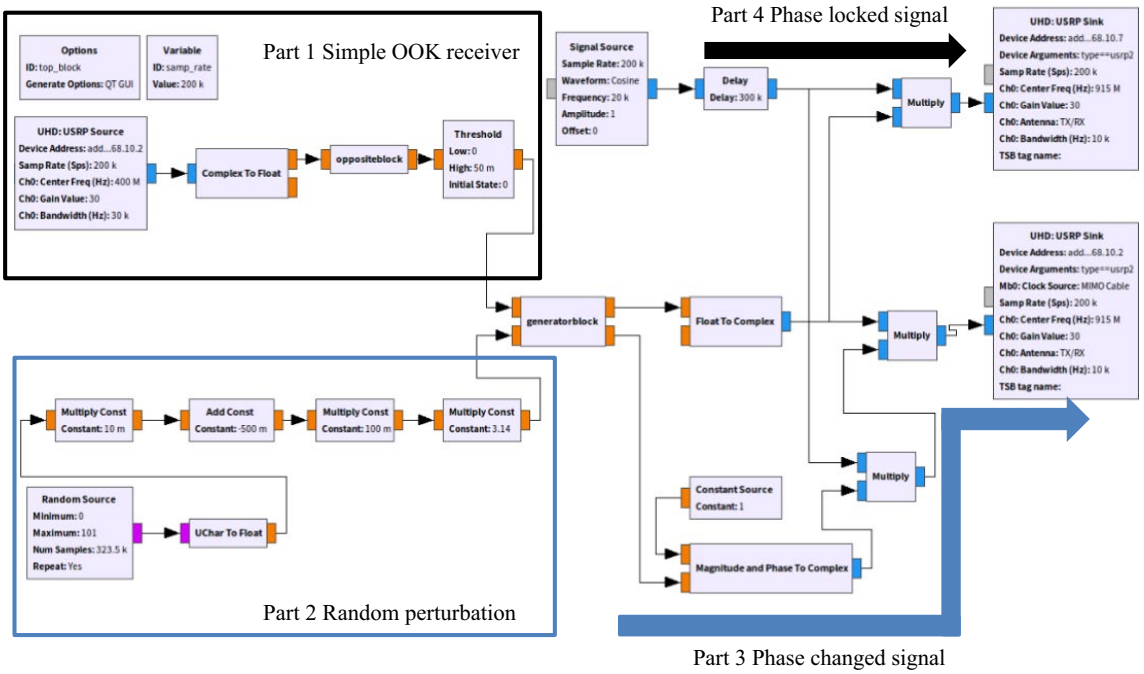

FIGURE 7 Flow of the beamforming process at each ETx

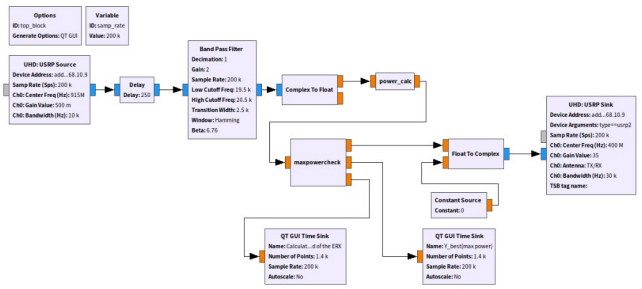

FIGURE 8 Flow of the feedback operation at the ERx

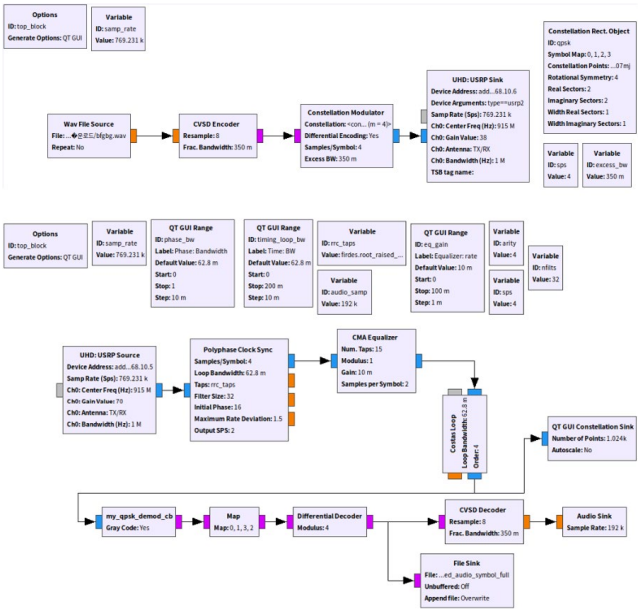

FIGURE 9 Flow graphs of the ITx (top) and the IRx (bottom)

Figure 9. We note that the feedback operation for the IRx can be implemented similarly to the ERx in Figure 8. In what follows, to demonstrate the validity of the implementation, we analyze the behavior of the experimentally measured data while changing the number of antennas and DBF algorithms.

In Figure 10, the energy signal waveforms received at the ERx and at the IRx are, respectively, shown when various DBF algorithms (ie, (A) Algorithm 1, (B) Algorithm 2, and (C) Algorithm 3 with $P_{\text{update}} = 0.7$) are applied. In Figure 10A, Algorithm 1 leads to a large energy signal RSS at the ERx, but it also incurs a large interference at the IRx, which coincides with the observation from the computer simulations in Section 4. Likewise, in Figure 10B, Algorithm 2 results in a small energy signal RSS (ie, low interference) at the IRx with decreased transferred energy at the ERx. In Figure 10C, when Algorithm 3 with $P_{\text{update}} = 0.7$ is applied, the RSS at the ERx is comparable to that obtained with Algorithm 1, but the interference power at the IRx is much smaller than that obtained with Algorithm 1, which is also coincides with the discussion on the trade-off curve between the received signal power at the ERx and the achievable rate at the IRx in Section 4. We note that if we increase the number of ETxs, the interference at the IRx can be further reduced, while the energy signal is magnified.

To verify the performance of the proposed scheme in a more practical environment, we also measured the harvested energy by exploiting the P2110 board with a rectenna, an off-the-shelf energy harvesting device. In Figure 11A, when a single ETx

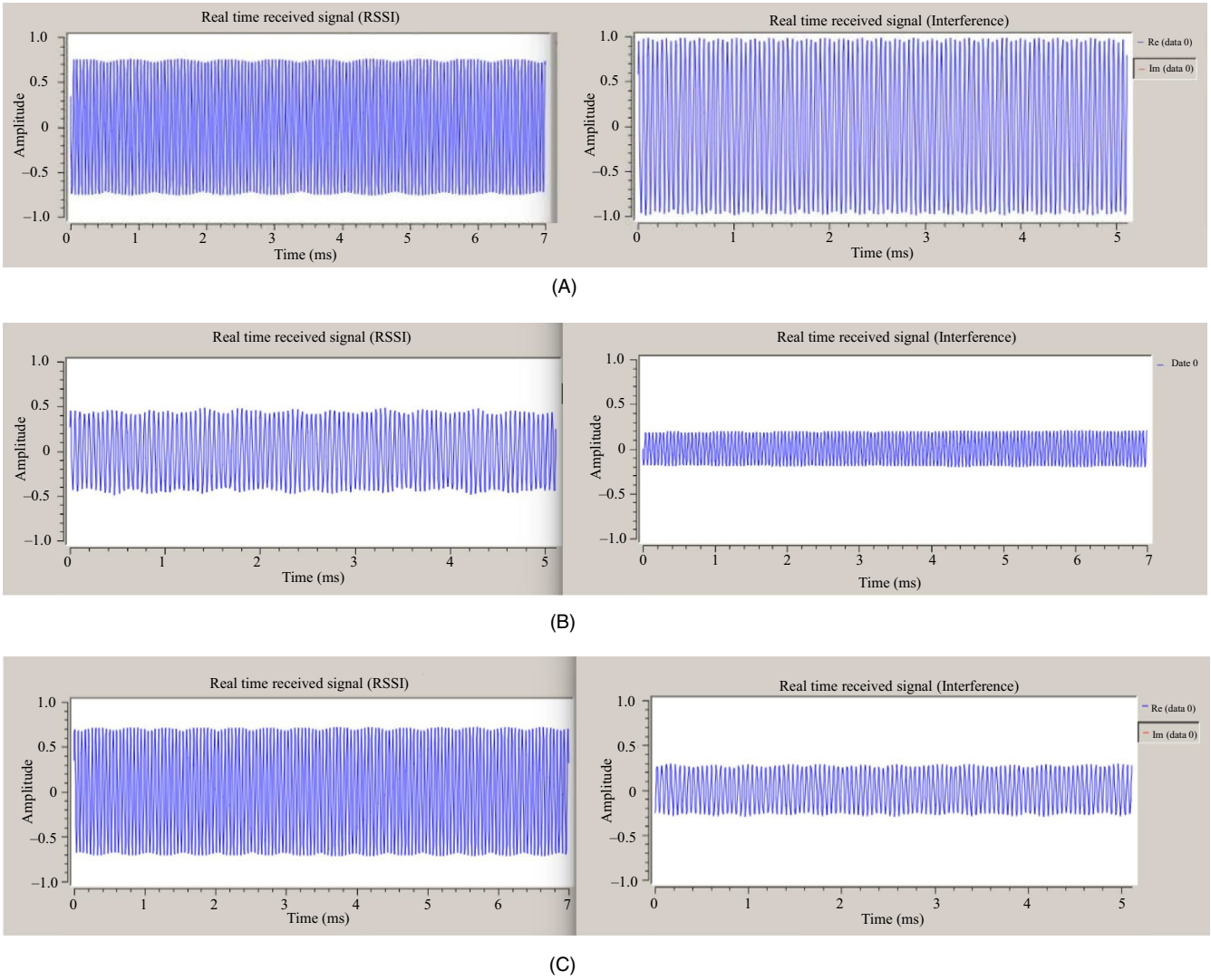

FIGURE 10 Energy signal waveforms received at the ERx (left) and IRx (right) with (A) Algorithm 1, (B) Algorithm 2, and (C) Algorithm 3 with $P_{\text{update}} = 0.7$

(consisting of the N210 with a WBX board and a vertical antenna) transmits the energy signal to the ERx (implemented by exploiting a P2110 board), 0.74 mW can be harvested at the ERx by the P2110. In Figure 11B, when Algorithm 1 is applied with two ETxs, 1.97 mW is harvested, which is enough to power an LED on the P2110 board (note that if more than 0.04 mW is harvested, the LED on the P2110 can be powered [17]). In Figure 11C, when Algorithm 2 is applied with two ETx, the interference power is harvested at the IRx by collocating the P2110 board with the IRx. Interestingly, because Algorithm 2 minimizes the interference at the IRx, the harvested power is much smaller than it is with a single ETx (Figure 11A).

In Figure 12, the constellation points of the received information signal at the IRx are shown when (A) there are no ETxs, (B) there are two ETxs with no beamforming, and (C) there are two ETxs with Algorithm 3. We can see that when there are no ETxs, the constellation points are clustered well around the QPSK points. In contrast, when there are two ETxs with no beamforming, the

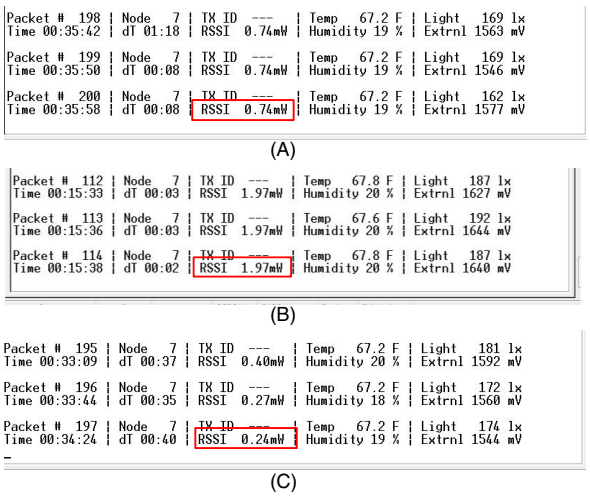

FIGURE 11 Harvested energy at P2110 board with a rectenna (A) at the ERx when a single ETx is exploited, (B) at the ERx when two ETxs with Algorithm 1 is exploited, and (C) at the IRx when two ETxs with Algorithm 2 is exploited

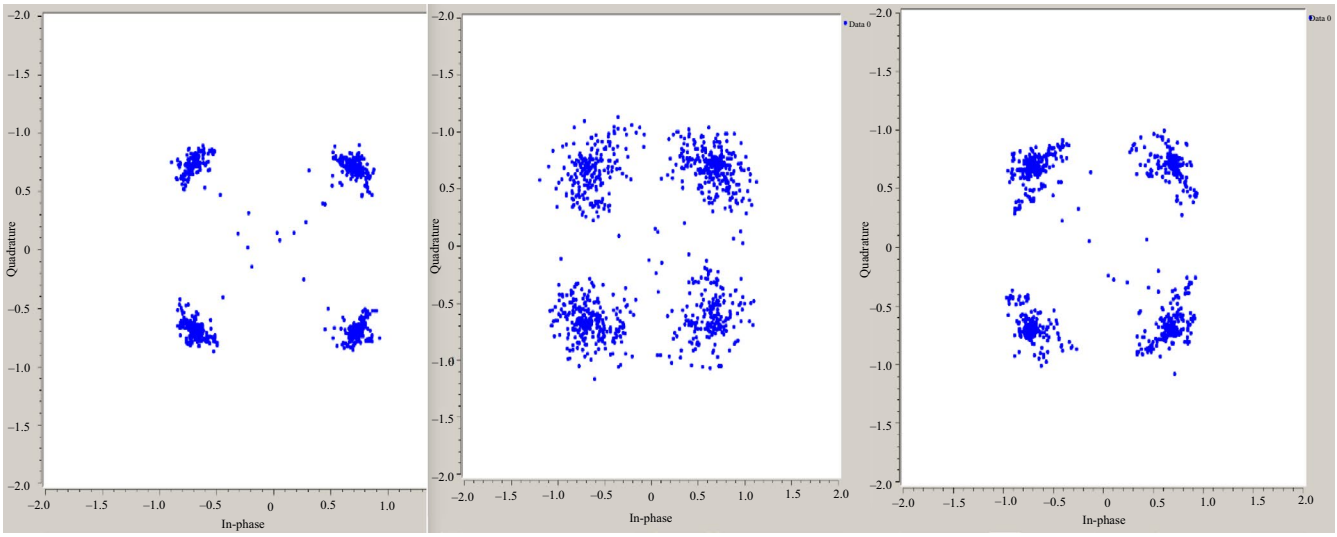

FIGURE 12 Constellation point of the received information signal at the IRx when (A) there are no ETxs, (B) there are two ETxs with no beamforming, and (C) there are two ETxs with Algorithm 3

constellation points are widely scattered due to the large interference from the ETxs. Figure 12C shows that when the proposed beamforming algorithm is applied, the constellation points are clustered well by reducing the interference at the IRx, which coincides with the observations in Figures 10 and 11.

6 | CONCLUSION

In this paper, we proposed one-bit feedback-based DBF algorithms in the interference channel where the information transfer network and the power transfer network coexist in the same frequency spectrum band. The DBF that maximizes the transferred energy to the ERx causes large interference at the IRx, while the DBF that minimizes the interference at the IRx cannot effectively transfer the energy to the ERx. Accordingly, we propose the DBF jointly maximizing the energy transferred to the ERx and minimizing the interference at the IRx in a stochastic way, where multiple ETxs determine their phases of the energy signal based on one-bit feedback reports from the ERx/IRx without sharing information among the distributed transmit nodes. Through a computer simulation, we identified the trade-off between the harvested energy and the achievable rate. Based on this trade-off, we proposed the optimal transmission strategy such that the harvested energy at the ERx is maximized without sacrificing the achievable rate at the IRx. We also implemented the proposed DBF system using GNU radio, USRP, and a P2110 board with a rectenna.

ORCID

Jaehyun Park https://orcid.org/0000-0001-5327-9111

REFERENCES

1. S. C. Lee et al., *Design and implementation of wireless sensor based-monitoring system for smart factory*, in Proc. Int. Conf. Comput. Sci. Applicat. (Kuala Lumpur, Malaysia), 2007, pp. 584–592.
2. B. Holfeld et al., *Wireless communication for factory automation: an opportunity for LET and 5G systems*, IEEE Commun. Mag. **54** (2016), 36–43.
3. A. Gonga, O. Landsiedel, and M. Johansson, *MobiSense: Power-efficient micro-mobility in wireless sensor networks*, in Proc. IEEE Int. Conf. Distrib. Comput. Sens. Syst. (Barcelona, Spain), June 2011, pp. 1–8.
4. J. Ren et al., *RF energy harvesting and transfer in cognitive radio sensor networks: Opportunities and challenges*, IEEE Commun. Mag. **56** (2018), 104–110.
5. H. Ju, Y. Lee, and T.-J. Kim, *Full-duplex operations in wireless powered communication networks*, ETRI J. **39** (2017), 794–802.
6. S. Lee, R. Zhang, and K. Huang, *Opportunistic wireless energy harvesting in cognitive radio networks*, IEEE Trans. Wirel. Commun. **12** (2013), 4788–4799.
7. J. Park and B. Clerckx, *Joint wireless information and energy transfer in a K-user MIMO interference channel*, IEEE Trans. Wireless Commun. **13** (2014), 5781–5796.
8. J. Park and B. Clerckx, *Joint wireless information and energy transfer with reduced feedback in MIMO interference channels*, IEEE J. Selected Areas Commun. **33** (2015), 1563–1577.
9. J. Park et al., *An analysis of the optimum node density for simultaneous wireless information and power transfer in Ad Hoc networks*, IEEE Trans. Veh. Technol. **67** (2018), 2713–2726.
10. R. Mudumbai et al., *Distributed transmit beamforming: Challenges and recent progress*, IEEE Commun. Mag. **47** (2009), 102–110.
11. R. Mudumbai et al., *Distributed transmit beamforming using feedback control*, IEEE Trans. Inf. Theory **56** (2010), 411–426.
12. S. Song et al., *Improving the one-bit feedback algorithm for distributed beamforming*, in Proc. IEEE Wireless Commun. Netw. Conf. (Sydney, Australia), Apr. 2010, doi: 10.1109/WCNC.2010.5506562.

13. F. Quitin et al., *Demonstrating distributed transmit beamforming with software-defined radios*, in Proc. IEEE Int. Symp. World Wireless, Mobile Multimedia Netw. (San Francisco, CA, USA), June 2012, doi: 10.1109/WoWMoM.2012.6263729.
14. M. M. Rahman et al., *Fully wireless implementation of distributed beamforming on a software-defined radio platform*, in ACM/IEEE Int. Conf. Inf. Process. Sensor Netw. (Beijing, China), Apr. 2012, 10.1109/IPSN.2012.6920945.
15. E. Blossom, *GNU radio: Tools for exploring the radio frequency spectrum*, Linux Journal **122** (2004), 2004.
16. Reserch, *Ettus, USRP N200/N210 networked series*, Moun-tain Viewi CA: Ettus Research, 2012.
17. Datasheet, Product, *P2110-915MHz RF powerharvester receiver*, Powercast Corporation, Available at www.powercastco.com/PDF/P2110-datasheet.pdf.
18. M. Chowdhury and A. Goldsmith, *Capacity of block Rayleigh fading channels without CSI*, in Proc. IEEE Int. Symp. Inf. Theory (Barcelona, Spain), July 2016, pp. 1884–1888.
19. Y. Zhu and D. Guo, *The degrees of freedom of isotropic MIMO interference channels without state information at the transmitters*, IEEE Trans. Inf. Theory **58** (2012), 341–352.
20. D. Tse and P. Viswanath, Fundamentals of wireless communication, Cambridge University Press, USA, 2005.
21. Guided Tutorial GRC, https://wiki.gnuradio.org/index.php/Guided_Tutorial_PSK_Demodulation

AUTHOR BIOGRAPHIES

Yong-Gi Hong received his BS degree in electronic engineering from Pukyong National University, Busan, Rep. of Korea, in 2020. His research interests include signal processing for wireless communications and radar systems, simultaneous wireless information and power transfer systems, and machine learning for communication systems.

SeongJun Hwang received his BS degree in electronic engineering from Pukyong National University, Busan, Rep. of Korea, in 2020. His research interests include communication signal processing, orthogonal frequency division modulation radar, and machine learning for communication systems.

Jiho Seo received his BS degree in electronic engineering from Pukyong National University, Busan, Rep. of Korea, in 2020. His research interests include signal processing in automotive radar and machine learning for radar imaging.

Jonghyeok Lee received his BS and MS degrees in electronic engineering from Pukyong National University, Busan, Rep. of Korea, in 2018 and 2020, respectively. His research interests include communication signal processing, wireless powered sensor networks, radar signal processing for automotive systems, and machine learning for radar and communication systems.

Jaehyun Park received his BS and PhD (MS-PhD joint program) degrees in electrical engineering from the Korea Advanced Institute of Science and Technology, Daejeon, Rep. of Korea, in 2003 and 2010, respectively. From 2010 to 2013, he was a senior researcher at the Electronics and Telecommunications Research Institute, where he worked on transceiver design and spectrum sensing for cognitive radio systems. From 2013 to 2014, he was a postdoctoral research associate in the Electrical and Electronic Engineering Department at Imperial College London, London, UK. He is now an associate professor at the Electronic Engineering Department at Pukyong National University, Busan, Rep. of Korea. His research interests include signal processing for wireless communications and radar systems, with focus on detection and estimation for multiple input multiple output (MIMO) systems, MIMO radar, cognitive radio networks, and joint information and energy transfer.